



**AMERICAN SOCIETY FOR METALS**  
**Metals Park, Ohio 44073**

**Metals/Materials Technology Series**

**ULTRASONIC CHARACTERIZATION OF  
POROSITY IN POWDER METALS**

**S. Howard, J. Tani, H. Arnold, H. Schwetlick,  
Wolfgang Sachse**

Department of Theoretical and Applied Mechanics  
Cornell University  
Ithaca, NY 14853

**1984 ASM Metals Congress**  
**Detroit, Michigan**  
**15-20 September 1984**

**8408-025**

No part of this paper may be reproduced, stored in a retrieval system, or transmitted, in any form or by any means, electronic, mechanical, photocopying, recording, or otherwise, without the prior written permission of the publisher.

Nothing contained in this paper is to be construed as a grant of any right of manufacture, sale, or use in connection with any method, process, apparatus, product, or composition, whether or not covered by letters patent or registered trademark, nor as a defense against liability for the infringement of letters patent or registered trademark.

8408-025

## ULTRASONIC CHARACTERIZATION OF POROSITY IN POWDER METALS

S. Howard, J. Tani, H. Arnold, H. Schwetlick,  
Wolfgang Sachse

Department of Theoretical and Applied Mechanics  
Cornell University  
Ithaca, NY 14853

### ABSTRACT

We present preliminary results of a project aimed at investigating ultrasonic techniques to measure the bulk density, pore size, and spatial variation of porosity in powder metal specimens. Specific techniques considered are ultrasonic wavespeed, attenuation and wave dispersion measurements, and the identification of spectral features in the amplitude spectra. Also discussed is the inverse medium problem for reconstructing the acoustic impedance profile along the direction of wave propagation in a specimen.

The advantages of near net-shape fabrication of complex-shaped parts from powder metals has long been recognized. The strength and moduli of such parts, never as high as an equivalent part machined from a solid metal, is a strong function of their density [1,2]. Controlling the strength is not only the total void fraction but also its shape and distribution [2]. The in situ non-destructive measurement of material density of powder metal parts is most readily achieved by x-ray radiographic techniques, eddy currents and mechanical vibrations and ultrasonic wave propagation measurements. It is the latter which are considered in this paper.

Several techniques for ultrasonic porosity measurements in powder metal specimens have been proposed. Among the first used were direct wavespeed measurements. Using pulse-echo, time-of-flight measurements, Brockelman [3] established a correlation between longitudinal wave velocity and tensile strength in sintered iron powders which was also related to the pressing direction in the specimens. In another test, the ultrasonic wavespeed measurements were shown to correlate with x-ray density measurements made along the central region of a

3.5-inch bar of sintered steel. Later, Papadakis and Petersen [4], using ultrasonic velocity measurements along different directions in briquetted and sintered specimens of steel powders, established a correlation between wavespeed and density. Other investigators have attempted to establish a relationship between ultrasonic attenuation and the porosity of a material. However, up to now, most measurements appear to have been restricted to porous rocks. A recent example is the work by Winkler [5] who measured attenuation and phase velocity spectra in sedimentary rocks under high pressure. Other work appears to have focused on measurements in two-phase materials. The work of Latiff and Fiore [6] was on a model material consisting of Cu spheres imbedded in an elastically isotropic polymethylmethacrylate (PMMA) matrix. When attempts were made to interpret the data with the multiple scattering theory developed by Waterman [7], only qualitative agreement was found.

Most of the recent work may be classified under the heading of ultrasonic spectral feature identification. In this area, two approaches have been pursued. Gubernatis and Domany [8] developed a theoretical model of elastic wave scattering to establish the relationship between the average pore radius and a frequency peak or transition in the spectrum of the scattered signals. They also showed the connection between the magnitude of this amplitude and the pore concentration. In the work of Tittman, et al [9], the focus was on the determination of the size and concentration of pores in IN-100 alloy from the slope of the backscattered ultrasonic amplitude spectrum. In two samples, the average pore size recovered from ultrasonic measurements was in agreement with the values determined from quantitative microscopy measurements. In the analytical approach, developed by Sayers and Smith [10], a relationship between porosity and ultrasonic wave dispersion effects is established which can be determined from the amplitude or phase

spectra of the ultrasonic echoes.

## EXPERIMENTS

Our research was conducted on hot-pressed, porous powder samples of iron, copper and aluminum. After fabrication, each sample was machined flat into the shape of a disk of about 2.54 cm in diameter and polished. The samples ranged in thickness from 3 to 6 mm and were flat to within 10.0  $\mu\text{m}$  (0.0004 inches). There were seven specimens of aluminum, six of iron and nine of copper. The specimen densities were determined from weight and volume measurements. The sintered aluminum powder specimens spanned a density range from less than 1.97  $\text{g/cm}^3$  to 2.69  $\text{g/cm}^3$ , corresponding to porosities ranging from 1.4% to 27%. The densities of the copper specimens ranged from 5.44  $\text{g/cm}^3$  to 8.75  $\text{g/cm}^3$ , corresponding to porosities ranging from 2.4% to 39%, while the iron powder specimens ranged in density from 4.87  $\text{g/cm}^3$  to 7.72  $\text{g/cm}^3$ , corresponding to porosities ranging from 2.0% to 38%.

The ultrasonic measurements were made using a broadband ultrasonic system in which highly-damped, longitudinal and shear piezoelectric transducers of varying center frequencies were shock excited and the detected echoes were amplified and processed. Both time-of-flight (velocity) and amplitude (attenuation) measurements were made. In the first experiments, the time-of-flight measurements were made to a resolution of approximately 20 nsec with a digital oscilloscope system. Preliminary measurements of the spatial variation of velocity were made with an immersion transducer moved in a rectangular grid pattern over the test specimen immersed in water. The time-of-flight was measured using a microprocessor-controlled time-interval counter. In these experiments, each data point represented the average of  $10^3$  time-interval determinations.

Measurement of the dispersion of ultrasonic pulses in a solid can be conveniently made using the phase spectroscopy technique described by Sachse and Pao [11]. In this technique, a broadband ultrasonic pulse is input into a specimen from a transducer and the signal received after propagating a distance  $L$  through a specimen is recorded either with the same transducer acting as a receiver or a second, receiving transducer. Both input and output signals are Fourier-transformed into the frequency-domain and their respective, unwrapped phase functions,  $\phi$  and  $\phi_0$  are determined. From the difference of these, the dispersion relation can be determined according to

$$k(\omega) = (\phi(\omega) - \phi_0(\omega)) / L \quad (1)$$

From this the phase and group velocities are found, where

$$v_{\text{phase}} = \omega / k = \omega L / (\phi(\omega) - \phi_0(\omega)) \quad (2a)$$

$$v_{\text{group}} = \partial\omega / \partial k = L [d\phi/d\omega]^{-1} \quad (2b)$$

Ultrasonic attenuation measurements were made using the buffer-rod technique described by Papadakis [12]. In this technique, a buffer rod is attached to the test specimen and the broadband, buffer-specimen echo,  $A(t)$ , and two successive specimen echoes,  $B(t)$  and  $C(t)$ , are analyzed in the frequency-domain. This permits determination of the reflection coefficient of the buffer-specimen interface and the attenuation of the test piece, independent of the excitation amplitude or the attenuation of the buffer rod. The frequency-dependent reflection coefficient and attenuation of the specimen is given by

$$R(f) = [\bar{A}\bar{C} / (\bar{A}\bar{C} - 1)]^{\frac{1}{2}} \quad (3a)$$

$$\alpha(f) = 1 / L \ln [R(f)/\bar{C}] \quad (3b)$$

where  $\bar{A}(f) = A(f)/B(f)$  and  $\bar{C}(f) = C(f)/B(f)$ . The value obtained from evaluation of Eq. (3a) can be compared with the expected value for the reflection coefficient

$$R = \frac{\rho_s c_s - \rho_b c_b}{\rho_s c_s + \rho_b c_b} \quad (4)$$

## RESULTS

The results of wavespeed measurements using longitudinal and shear waves in sintered aluminum powder specimens is shown in Figs. 1(a) and (b). The longitudinal wavespeed measurements shown were made with two transducers possessing different center frequencies. A linear least-squares fit was made to the wavespeed data. The solid line and open data points in Fig. 1(a) correspond to data taken with a 2.25 MHz transducer generating a pulse with center frequency near 2 MHz. The other data (dashed line, crosses) corresponds to measurements made with a 10 MHz transducer generating a pulse with center frequency near 7 MHz. The average slope of these two data sets was 0.420  $\text{cm}/\mu\text{sec}/\text{g/cm}^3$ . The shear wave measurements shown in Fig. 1(b) were made with pulses whose center frequency was near 5 MHz. The slope of the least-squares fit line was 0.160  $\text{cm}/\mu\text{sec}/\text{g/cm}^3$ . The results of similar experiments made in iron powder specimens is shown in Figs. 2(a) and (b). The average of the slopes of the two least-squares linear fits to the longitudinal wavespeed/density data is 0.104  $\text{cm}/\mu\text{sec}/\text{g/cm}^3$ ; for shear waves the slope is 0.0487  $\text{cm}/\mu\text{sec}/\text{g/cm}^3$ . The results of the corresponding experiments with copper specimens are shown in Figs. 3(a) and (b). The longitudinal and shear wave/density slopes are determined to be 0.0774 and 0.0285  $\text{cm}/\mu\text{sec}/\text{g/cm}^3$ , respectively. We note

that the variation in wavespeed with density is highest for aluminum and lowest for copper.

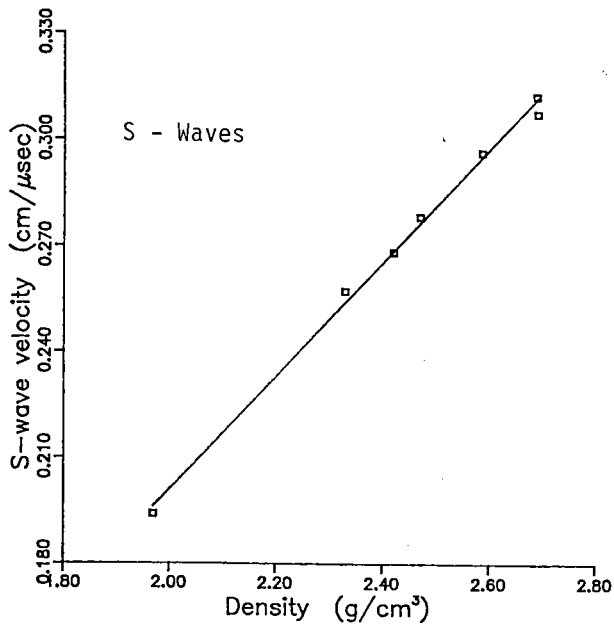
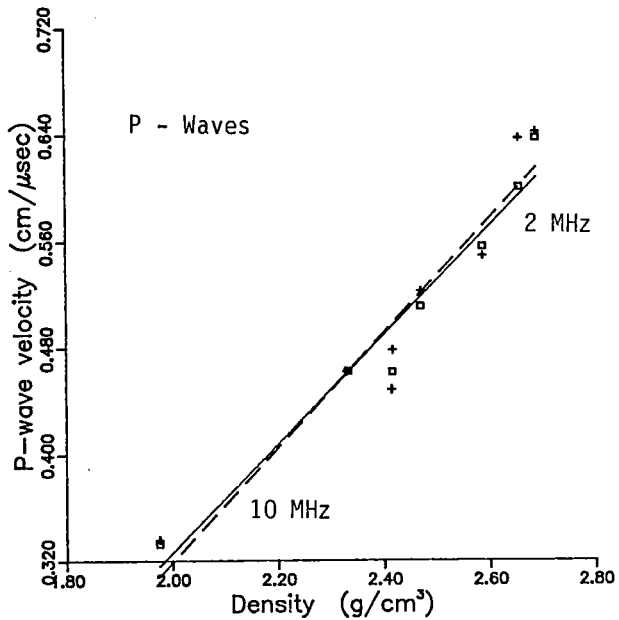


Figure 1(a)-(b) - Hot-pressed Aluminum

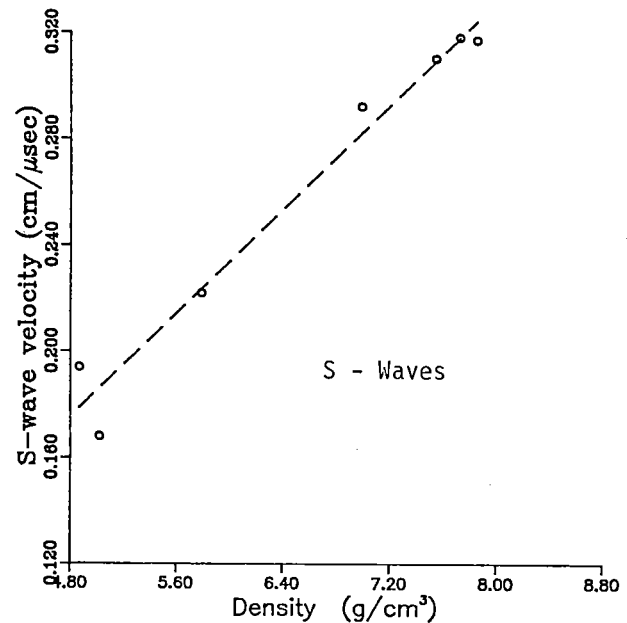
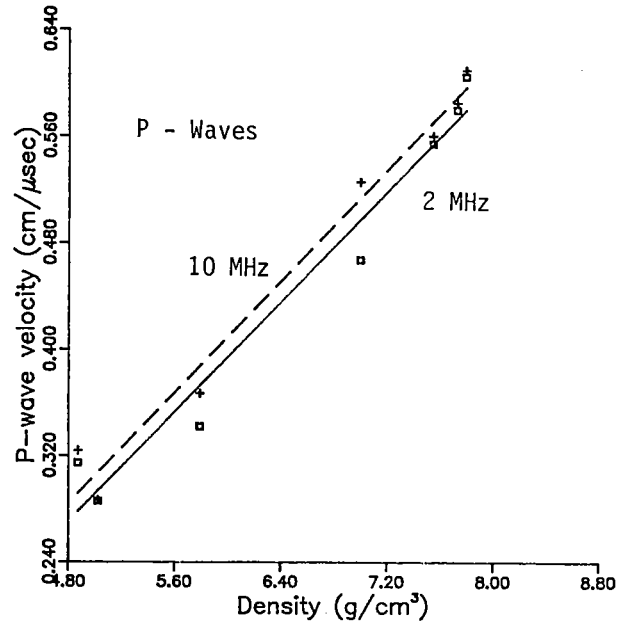


Figure 2(a)-(b) - Hot-pressed Iron

The importance of the results shown in Figs. 1 - 3 is that they provide a means for converting wavespeed measurements to density measurements for a specific material. Because of the measured linear relationship between wavespeed and density, the values of slope and intercept should be sufficient to convert ultrasonic wavespeed data into a density determination. To evaluate the reliability of this procedure, we calculated the error in density expected when using our measured data as input to the conversion algorithm. The root-mean-square deviation in longitudinal

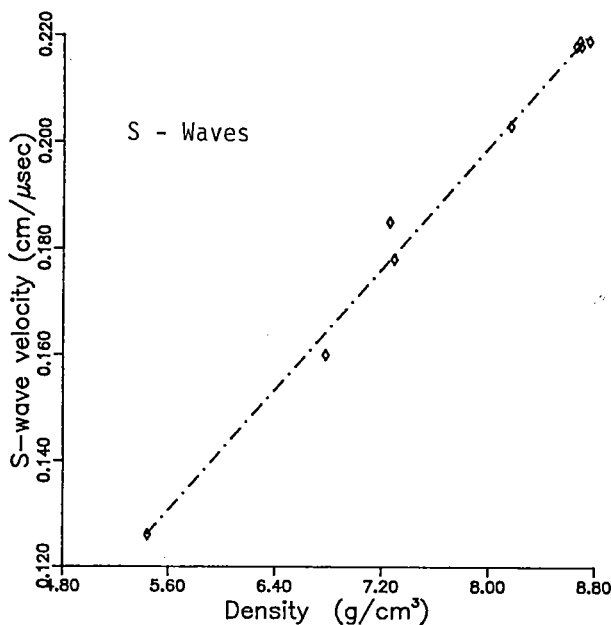
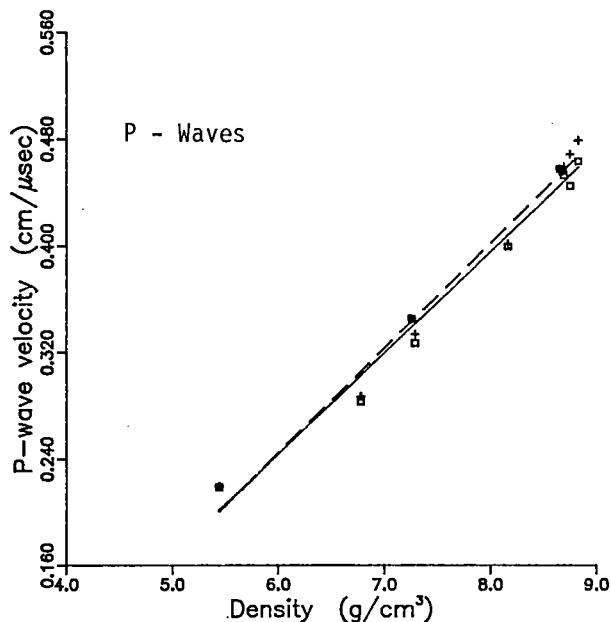


Figure 3(a)-(b) - Hot-pressed Copper

wavespeed,  $\Delta c$ , was evaluated for the wavespeed data shown in Figs. 1(a)-3(a) and the corresponding variation in density,  $\Delta \rho = \Delta c/m$  was then determined for each material, where  $m$  is the slope of the lines in the figures. Dividing  $\Delta \rho$  by the maximum density for each material, we obtained numbers corresponding to the measurement resolution with the 2.25 Mhz and the 10 MHz transducer data sets. Another two sets of data were obtained using a 5 MHz longitudinal wave transducer. The four sets of longitudinal wave data gave resolution values ranging from 1.74-2.37%, 2.16-2.92% and 1.58-1.90% for aluminum, copper, and iron, respectively. It is possible that

these values can be improved by better transducer/specimen coupling techniques or by using non-contact transduction techniques.

Two sample results of phase velocities determined with the phase spectroscopy technique are shown in Figs. 4(a) and (b). The longitudinal wave results were obtained by using a 10 MHz broadband transducer. The Fourier amplitudes were sufficiently strong at frequencies up to 50 MHz to be useable for the analysis. In agreement with the multi-transducer experiments, it is seen that the wavespeed is found to be essentially frequency-independent for all the specimens tested. Similar experiments with shear waves also showed that the pulses were not dispersed since the wavespeeds were found to be frequency-independent. Sample results from various specimens, spanning the different materials and porosities are shown in Fig. 4(b). The average velocity values are in agreement with those determined from direct time-of-flight measurements.

As described in the previous section, the attenuation measurements were made with a buffer rod technique in which the buffer rod was fused quartz. The measurements were made with four different broadband transducers of nominal frequencies of 2.25, 5, 10 and 50 MHz. Shown in Fig. 5 is the specimen to buffer signal ratio obtained in an iron-powder specimen. The result obtained from the 50 MHz transducer is not shown since its ratio differed appreciably from the others.

The determination of the frequency-dependent reflection coefficients from the amplitude ratios  $A(f)$  and  $C(f)$  was made according to Eq. 3(b). Two sample results for iron specimens attached to quartz buffer rods are shown in Figs. 6(a) and (b). Also shown, as a dashed line, are the expected reflection coefficients computed from density and wavespeed values for the particular specimens shown. Although these results were computed without incorporating any corrections for diffraction or band limitations of the excitation pulse or transducer response, even at the mid-frequency points, near 2 MHz, the difference between expected and measured values was significant. For this reason, no attenuation values were evaluated. This result raises questions regarding the reliability of amplitude measurements which seriously affect any porosity determination procedure based on an attenuation measurement.

### AL-POWDER SPECIMENS (P-Wave)

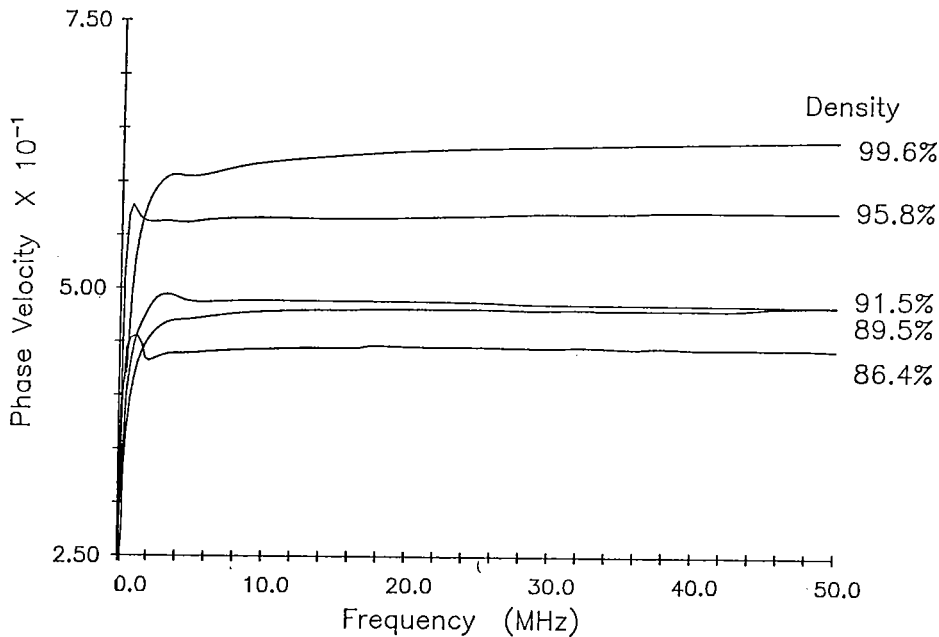


Figure 4(a) - Longitudinal phase velocity in Aluminum.  
(Units: cm/μsec)

### POWDER SPECIMENS: Al;Cu;Fe (S-Wave)

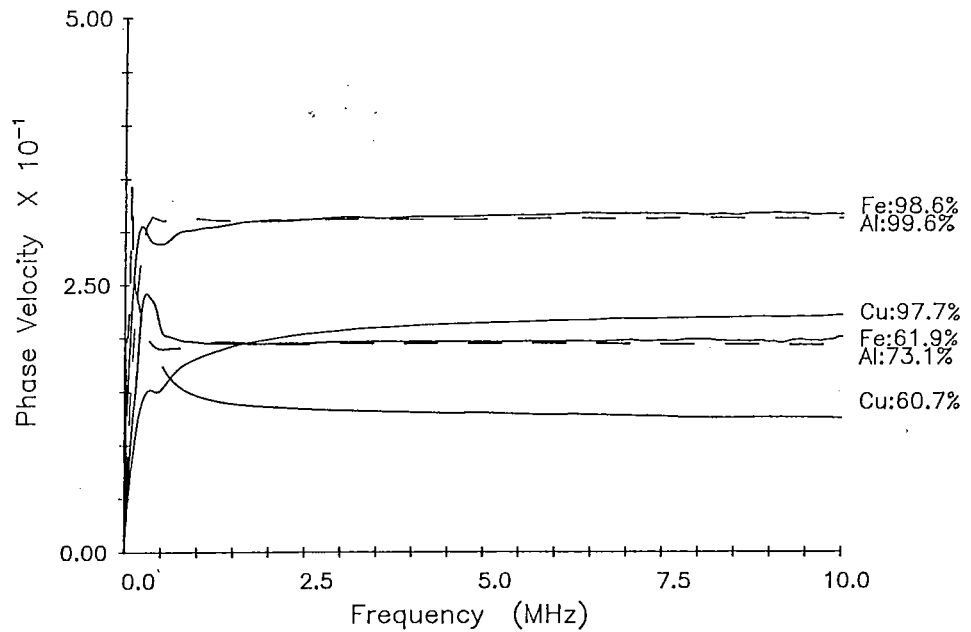


Figure 4(b) - Shear wave phase velocity in Al, Cu and Fe hot-pressed specimens.  
(Units: cm/μsec)

Two examples of the determination of two dimensional spatial variations of porosity are shown in Figs. 7(a) and (b). These two specimens were unfired Al-powder briquettes, pressed at 20 ksi and 27 ksi with a resulting porosity of 7.3% and 5.4% respectively. The specimens were polished flat to within 10 μm (0.0004 inches) which corresponds to a possible variation in the travel time of approximately

2.0 nsec. It is seen that there is a significant variation above this value across the cross section of the disks. The variation was almost 20 nsec for the more porous specimen corresponding to a higher wavespeed near the edge of the briquette than at its center. A similar but not as pronounced effect is seen with the less porous sample.

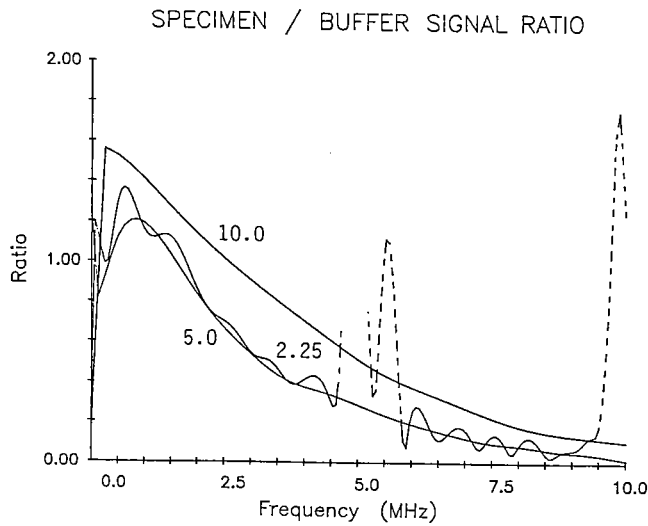
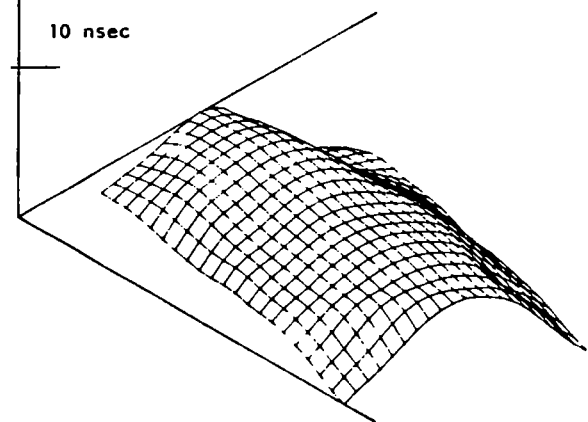


Figure 5 - P-wave Signal in Hot-Pressed Fe, 88%

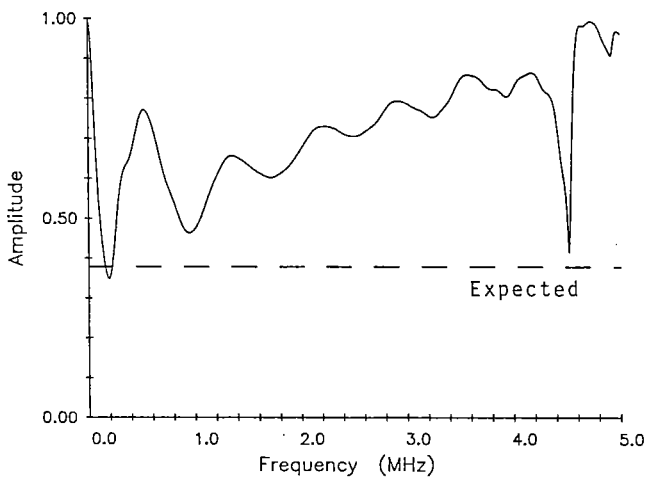
Porosity = 0.073

Wavespeed = 0.52 cm/ $\mu$ sec



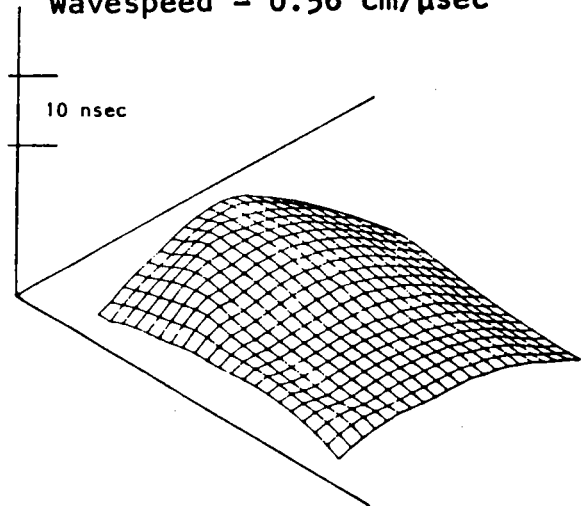
20 ksi Compaction

QUARTZ/IRON (88.8%) REFLECTION COEFFICIENT



Porosity = 0.054

Wavespeed = 0.56 cm/ $\mu$ sec



27 ksi Compaction

QUARTZ/IRON (98.1%) REFLECTION COEFFICIENT

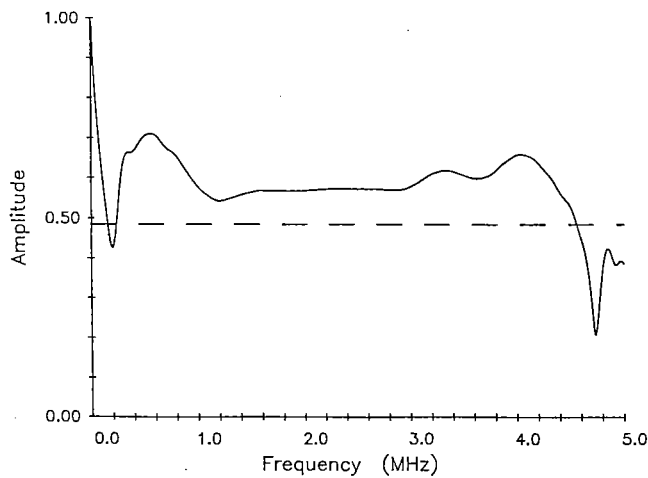


Figure 7(a)-(b) - Time-of-Flight in Al-powder Briquettes: (a) - 20 ksi; (b) - 27 ksi Compaction

Figure 6(a)-(b) - Measured, Expected Reflection Coefficient; Iron/Quartz Interface

The determination of the density and wavespeed variation along the direction of propagation from measurement of input and output signals forms the basis of the inverse medium problem which has been the subject of much research. Algorithms for obtaining the solution of such problems when band-limited excitation signals corresponding to typical ultrasonic pulses are used are still being developed [13]. We show, therefore, the results of a simulation



experiment. As shown in Fig. 8(a) a specimen of length  $L$  was simulated which has in its interior a region of impedance 10% higher than the surrounding outer regions situated normal to the direction of wave propagation. The synthesized excitation pulse produced by a transducer is shown in Fig. 8(b) and the signal received by the same transducer is in Fig. 8(c). To make this simulation more realistic and to verify the stability of the inversion scheme which is based on the method of characteristics [14], broadband noise whose rms value was 30% of the peak signal amplitude was added to the received signal. The broadband noise signal was the actual signal obtained from a broadband ultrasonic preamplifier. The results shown in Fig. 8(d) are the reconstructed impedance profiles from the noise-free and the 30% noise added waveforms.

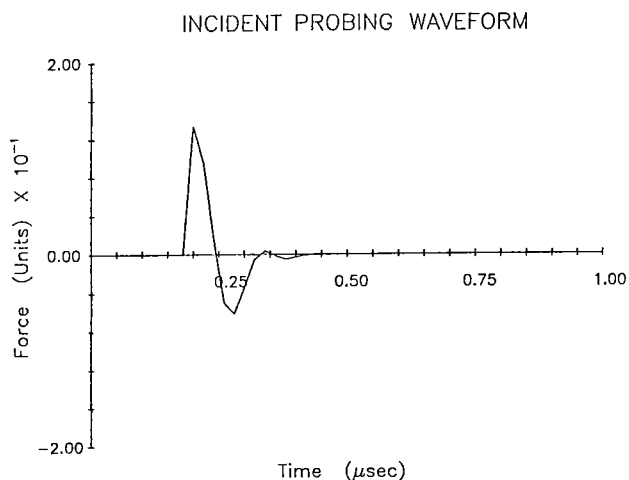
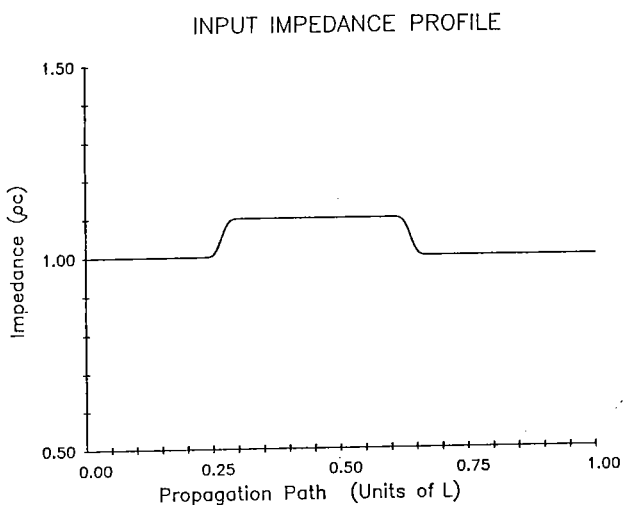


Figure 8 - Impedance Profile Reconstruction Simulation  
(a) Input Profile; (b) Probing Waveform

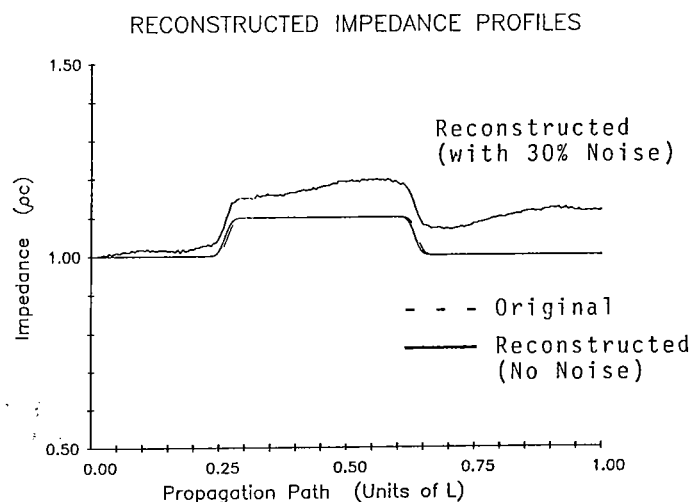
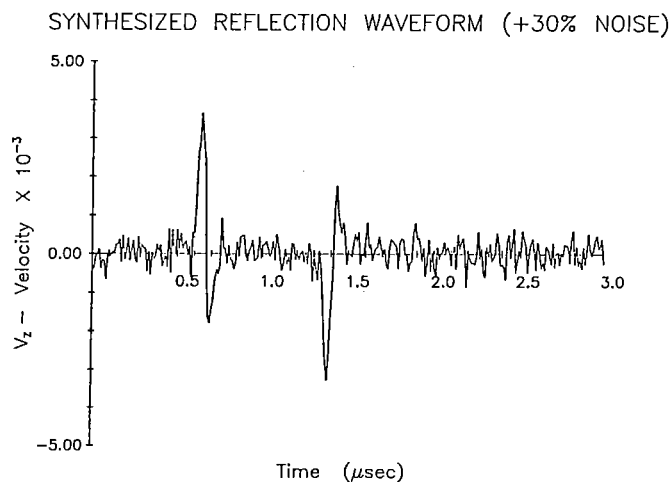


Figure 8 - Continued  
(c) - Synthesized Reflection Waveform

### CONCLUSIONS

We have reported results of ultrasonic longitudinal and shear wave measurements made in powder metal specimens of aluminum, iron and copper ranging in porosity from 1% to 39%. Ultrasonic time-of-flight (velocity) data were used to determine a relationship between density and longitudinal and shear wavespeeds. This relationship can be inverted to permit determination of the density or porosity of porous metal specimens. Using a simple error model, a density resolution was determined. It was established that errors in the wavespeed measurements lead to density variations of approximately 2% which are not resolvable. A more reproducible measurement technique is needed to yield resolution of smaller density variations.

Ultrasonic phase spectroscopy measurements showed that in the measured frequency range, the

wavespeeds are frequency-independent. Ultrasonic attenuation measurements were made with a buffer-rod technique. Based on a comparison between the recovered and expected wave reflection coefficients from the buffer/specimen interface, it was shown that amplitude and hence attenuation measurements cannot be made reliably.

A numerical simulation of the forward and inverse problem was made of a specimen which has in its interior a layer of material whose impedance is 10% greater than the outside layers. The synthesis shows that even with 30% added noise, an inversion scheme based on the method of characteristics can be used to recover the impedance profile of the specimen.

#### ACKNOWLEDGMENTS

This work was carried out under the Grants-in-Aid for Education Program of Bethlehem Steel Corporation with Dr. B. E. Droney project coordinator. Partial support was also obtained from the National Science Foundation through a grant to the Materials Science Center at Cornell University. This support is gratefully acknowledged. We thank also Mr. B. F. Addis for his care in preparing the specimens.

#### REFERENCES

1. W. D. Jones, Fundamental Principles of Powder Metallurgy, Edward Arnold Publ., Ltd., London (1960), pp. 839-844.
2. J. S. Hirschhorn, Introduction to Powder Metallurgy, Am. Powder Metall. Inst., New York (1969), pp. 253-261.
3. R. H. Brockelman, "Dynamic Elastic Determination of the Properties of Sintered Powder Metals", in: Advanced Experimental Techniques in Powder Metallurgy, Plenum Press, New York (1970), pp. 201-224.
4. E. P. Papadakis and B. W. Petersen, "Ultrasonic Velocity as a Predictor of Density in Sintered Powder Metal Parts", Materials Evaluation, **37**, 76-80 (1979).
5. K. W. Winkler, "Attenuation and Phase Velocity Spectra in Sedimentary Rocks under High Pressure", 1982 Ultrasonics Symposium Proceedings, Vol. 2, Inst. Electr. Electr. Eng., New York (1982), pp. 1054-1058.
6. R. H. Latiff and W. F. Fiore, "Ultrasonic Attenuation and Velocity in Two Phase Microstructures", J. Acoust. Soc. Am., **57**, 1441-1446 (1975).
7. P. C. Waterman and R. Truell, "Multiple Scattering of Waves", J. Math. Phys., **2**, 512-537 (1961).
8. J. E. Gubernatis and E. Domany, "Effects of Microstructure on the Speed and Attenuation of Elastic Waves: Some Results for Porous Materials", Wave Motion, **16**, 580-589 (1984).
9. B. R. Tittman, J. Ahlberg, K. W. Fertig, "Ultrasonic Microstructural Noise Parameters in a Powder Metal Alloy", in Review of Progress in Quantitative NDE, Vol. 3A, D. O. Thompson and D. E. Chimenti, Eds., Plenum Press, New York (1984), pp. 57-64.
10. C. M. Sayers and R. L. Smith, "The Propagation of Sound in Porous Media", Ultrasonics, **20**, 201-205 (1982).
11. W. Sachse and Y.-H. Pao, "On the Determination of Phase and Group Velocities of Dispersive Waves in Solids", J. Appl. Phys., **49**, 4320-4327 (1978).
12. E. P. Papadakis, "Ultrasonic Velocity and Attenuation Measurement Methods with Scientific and Industrial Applications", in Physical Acoustics, Vol. XII, W. P. Mason and R. N. Thurston, Eds., Academic Press, New York (1979), pp. 277-374.
13. Y.-H. Pao, F. Santosa and W. Symes, "Inverse Problems of Acoustic and Elastic Waves", in Inverse Problems of Acoustic and Elastic Waves, F. Santosa, Y.-H. Pao, W. Symes and C. Holland, Eds., SIAM, Philadelphia (1984), pp. 274-302.
14. F. Santosa and H. Schwetlick, "The Inversion of Acoustical Impedance Profile by the Method of Characteristics", Wave Motion, **4**, 99-110 (1982).